Journal of Applied Sciences

ISSN 1812-5654

science alert

ANSInet
an open access publisher
http://ansinet.com

Journal of Applied Sciences 12 (3): 221-232, 2012
ISSN 1812-5654 / DOI: 10.3923/jas.2012.221.232

Nonlinear Analysis of Concrete Structural Components Using Co-axial Rotating Smeared Crack Model

Mohammad Amin Hariri Ardebili, S. Mahdi S. Kolbadi, Masoud Heshmati and Hasan Mirzabozorg
Department of Civil Engineering, K. N. Toosi University of Technology, Tehran, Iran

Abstract: Simulation of concrete behavior in structural components and estimation of real crack profile under static and dynamic loads is one of the most interesting fields in structural engineering. In the present study, a co-axial rotating smeared crack model is proposed for mass concrete in 3D space. The advantages of this model are using variable shear transfer coefficient which is updated in each load step; utilizing an advanced failure criterion for concrete and ability of modeling concrete cracking in tension and also crushing in compression. The proposed model is verified considering concrete beams under concentrated loads and comparing the results with those available in the literature. In addition, a finite element model of prototype gravity dam-reservoir-foundation system is provided in order to investigation the nonlinear dynamic behavior of large concrete specimens considering fluid-structure-interaction. The responses of the dam as well as crack profiles are compared for constant and variable shear transfer coefficients under various types of dynamic loads. Results show great compatibility of numerical modeling and experimental tests. In addition, results confirm importance of shear transfer coefficients in dynamic analysis of concrete gravity dams.

Key words: Nonlinear analysis, increasing dynamic load, fluid-structure-interaction, rotating smeared crack model, shear retention factor

INTRODUCTION

Modeling behavior of concrete materials in structural components is one of the most interesting fields in structural engineering. Complex models are required in order to capture the nonlinear behavior that arises as the structure is loaded. Several researchers have introduced models in order to simulating the nonlinear behavior and also failure of concrete under static and dynamic loads. The methods based on Continuum Crack Model (CCM), Discrete Crack Model (DCM), Interface Crack Approach (ICA) and the method of constrains are samples of most favorite methods for numerical simulation of concrete behavior. Utilizing these methods in conjunction with analytical solutions depends on the complexities of the structures, material properties and the boundary conditions. Numerical models such as finite element; finite difference; finite volume; extended finite element and mesh free approaches are common methods for simulation of structural components and their behavior (Yu *et al*., 2008).

The DCM requires monitoring the response and modifying topology of the mesh corresponding to the current crack configurations at each state of loading. However, this approach explicitly represents the crack as a separation of nodes which is a more realistic representation of the opening crack. This model is also useful when the location and direction of cracks is recognizable before loading the structure. Hohberg (1990) studied the mechanism of joint elements under water pressure using DCM. Ahmadi and Razavi (1992) represented a finite element model of discrete cracks for modeling joints. They considered perfectly elastic-plastic behavior for joint in tension and linear elastic behavior in compression and shear. Ahmadi *et al*. (2001) introduced a nonlinear joint element with coupled tension-shear behavior for analysis of arch dams. Lotfi and Espandar (2004) used discrete crack method, non-orthogonal smeared crack and combination of them for seismic analysis of dams. Du and Tu (2007) combined explicit finite element method with transmitting boundary to study the effects of contraction joint opening in concrete dams.

The methods based on CCM are divided to two major groups, i.e., damage mechanics approach and smeared crack approach. In the smeared crack approach cracks and joints are modeled in an average sense by appropriately modifying the material properties at the integration points of regular finite elements. Smeared cracks are convenient when the crack orientations are not known beforehand, because the formation of a crack involves no re-meshing or new degrees of freedom.

Corresponding Author: Hasan Mirzabozorg, Vali-asr St., Mirdamad Intersection, P.O. Box 15875-4416, Tehran, Iran
Tel: +98 (21) 88779623 Fax: +98 (21) 88779476

Some researchers applied continuum damage mechanics to study the concrete behavior such as Sumarac *et al.* (2003), Labadi and Hannachi (2005), Contrafatto and Cuomo (2006), Grassl and Jirasek (2006), He *et al.* (2006), Cicekli *et al.* (2007) and Khan *et al.* (2007). Also, Mirzabozorg *et al.* (2004) utilized damage mechanics approach to conduct seismic nonlinear analysis of concrete gravity dams in 2D space including dam-reservoir interaction effects. Ardakanian *et al.* (2006) considered nonlinear seismic behavior of mass concrete in 3D space which is based on an anisotropic damage mechanics model.

Failure based on the smeared crack approach and classification of its branches were studied by Malvar and Fourney (1990), Weihe *et al.* (1998), Mosler and Meschke (2004) and Phama *et al.* (2006). Mirzabozorg and Ghaemian (2005) developed a model based on smeared crack approach in 3D space. In their study, they analyzed 3D models including dam-reservoir interaction effects and considered nonlinear behavior of the structure. In addition, Mirzabozorg *et al.* (2007) investigated non-uniform cracking in smeared crack approach for 3D analysis of concrete dams and Mirzabozorg *et al.* (2010) studied nonlinear behavior of concrete dams under non-uniform earthquake ground motion records.

In the present study, a co-axial smeared crack model was introduced in 3D space for crack analysis of concrete structural components under static and dynamic conditions. For this purpose an advanced failure criterion is utilized. Finite element model of a set of beams are studied for constant and variable shear transfer coefficient conditions. In addition, capability of the proposed method is investigated for considering the behavior of coupled structure-fluid-soil system under various load types.

CONSTITUTIVE LAW FOR CONCRETE

The proposed method for crack analysis of concrete structural components should be able to simulate the behavior of the element in various states as following; Pre-softening behavior; fracture energy conservation; nonlinear behavior during the softening phase and finally crack closing/reopening behavior. The following sub-sections represent a brief review on general concepts of these stages.

Pre-softening phase: Generally, the relationship of the stress and strain vectors at the pre-softening phase is given as:

$$\{\sigma\} = [D]_{elastic}\ \{\varepsilon\} \quad (1)$$

where, $[D]_{elastic}$ is the elastic modulus matrix; $\{\sigma\}$ and $\{\varepsilon\}$ are the vector of stress and strain components. The modulus matrix in elastic condition maybe defined for isotropic, orthotropic and anisotropic materials.

Softening phase: During the softening phase, the elastic stress-strain relationship is substituted with an anisotropic modulus matrix which corresponds to the stiffness degradation level in the three principal directions. In the present study, the secant modulus stiffness approach, SMS, is unitized for the stiffness formulation in which the constitutive relation is defined in terms of total stresses and strains, shown in Fig. 1.

The stiffness modulus matrix based on the smeared crack propagation model is given in Eq. 2. It is worth noting that the extracted modulus matrix is co-axial with the principal strains in the considered location within the cracked element:

$$[D]^{local}_{crack} = \begin{bmatrix} D_{11} & & & & & \\ D_{12} & D_{22} & & & sym. & \\ D_{13} & D_{23} & D_{33} & & & \\ 0 & 0 & 0 & D_{44} & & \\ 0 & 0 & 0 & 0 & D_{55} & \\ 0 & 0 & 0 & 0 & 0 & D_{66} \end{bmatrix} \quad (2)$$

Where:

$$\begin{aligned} D_{11} &= \frac{\eta_1 E\left(1-\upsilon^2\eta_2\eta_3\right)}{1-\upsilon^2\eta_1\eta_2-\upsilon^2\eta_2\eta_3-\upsilon^2\eta_1\eta_3-2\upsilon^3\eta_1\eta_2\eta_3} \\ D_{22} &= \frac{\eta_2 E\left(1-\upsilon^2\eta_1\eta_3\right)}{1-\upsilon^2\eta_1\eta_2-\upsilon^2\eta_2\eta_3-\upsilon^2\eta_1\eta_3-2\upsilon^3\eta_1\eta_2\eta_3} \\ D_{33} &= \frac{\eta_3 E\left(1-\upsilon^2\eta_1\eta_2\right)}{1-\upsilon^2\eta_1\eta_2-\upsilon^2\eta_2\eta_3-\upsilon^2\eta_1\eta_3-2\upsilon^3\eta_1\eta_2\eta_3} \\ D_{12} &= \frac{\upsilon\eta_1\eta_2 E\left(1+\upsilon\eta_3\right)}{1-\upsilon^2\eta_1\eta_2-\upsilon^2\eta_2\eta_3-\upsilon^2\eta_1\eta_3-2\upsilon^3\eta_1\eta_2\eta_3} \\ D_{23} &= \frac{\upsilon\eta_2\eta_3 E\left(1+\upsilon\eta_1\right)}{1-\upsilon^2\eta_1\eta_2-\upsilon^2\eta_2\eta_3-\upsilon^2\eta_1\eta_3-2\upsilon^3\eta_1\eta_2\eta_3} \\ D_{13} &= \frac{\upsilon\eta_1\eta_3 E\left(1+\upsilon\eta_2\right)}{1-\upsilon^2\eta_1\eta_2-\upsilon^2\eta_2\eta_3-\upsilon^2\eta_1\eta_3-2\upsilon^3\eta_1\eta_2\eta_3} \\ D_{44} &= \beta_{12} G \\ D_{55} &= \beta_{23} G \\ D_{66} &= \beta_{13} G \end{aligned} \quad (3)$$

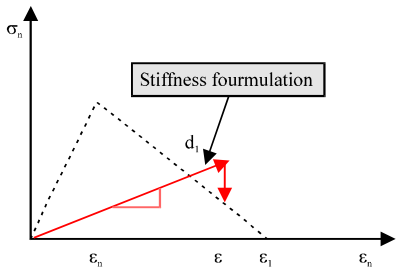

Fig. 1: SMS formulation of stiffness modulus matrix

where, η_1, η_2 and η_3 are the ratio of the softened Young's modulus in the three principal directions and the initial isotropic elastic modulus and β_{12}, β_{23} and β_{13} are shear re-tension factors corresponding to the principal directions given as:

$$\begin{aligned}
\beta_{12} &= \frac{1+\upsilon}{\Gamma}\left(\frac{\eta_1\varepsilon_1-\eta_2\varepsilon_2}{\varepsilon_1-\varepsilon_2}+\frac{\upsilon\eta_3(\eta_1-\eta_2)\varepsilon_3}{\varepsilon_1-\varepsilon_2}-\upsilon\eta_1\eta_2-2\upsilon^2\eta_1\eta_2\eta_3\right)\\
\beta_{23} &= \frac{1+\upsilon}{\Gamma}\left(\frac{\eta_2\varepsilon_2-\eta_3\varepsilon_3}{\varepsilon_2-\varepsilon_3}+\frac{\upsilon\eta_1(\eta_2-\eta_3)\varepsilon_1}{\varepsilon_2-\varepsilon_3}-\upsilon\eta_2\eta_3-2\upsilon^2\eta_1\eta_2\eta_3\right)\\
\beta_{13} &= \frac{1+\upsilon}{\Gamma}\left(\frac{\eta_1\varepsilon_1-\eta_3\varepsilon_3}{\varepsilon_1-\varepsilon_3}+\frac{\upsilon\eta_2(\eta_1-\eta_3)\varepsilon_2}{\varepsilon_1-\varepsilon_3}-\upsilon\eta_1\eta_3-2\upsilon^2\eta_1\eta_2\eta_3\right)\\
\Gamma &= 1-\upsilon^2\eta_1\eta_2-\upsilon^2\eta_2\eta_3-\upsilon^2\eta_1\eta_3-2\upsilon^3\eta_1\eta_2\eta_3
\end{aligned} \quad (4)$$

The constitutive matrix given in Eq. 2 is transformed to the global co-ordinate system as following:

$$[D]_{crack}^{global}=[T]^T[D]_{crack}^{local}[T] \quad (5)$$

where, [T] is the strain transformation matrix in 3D space. Based on the maximum strain reached in each principal direction, the secant modulus matrix is determined. Increasing the normal strain in each principal direction leads to reduction of the corresponding softened Young's modulus. Finally, when the maximum strain reaches the fracture strain, the considered Gaussian point within the element in the corresponding direction is fully cracked and its contribution in the stiffness matrix of the element is eliminated. Based on Eq. 2 to 5, any change in principal strains or their directions in each Gaussian point leads to an update requirement of the global constitutive matrix, $[D]_{crack}^{global}$. Satisfying the energy conservation principle in each Gaussian point leads to the fracture strain under static and dynamic loads:

$$\varepsilon_f=\frac{2G_f}{\sigma_0 h_c} \text{ and } \varepsilon_f^{'}=\frac{2G_f^{'}}{\sigma_0^{'} h_c} \quad (6)$$

where, h_c is the characteristic dimension of the considered Gaussian point and is assumed equal to the cubic root of the Gaussian point's volume contribution; σ_0 is the stress corresponding to the softening strain and G_f is the specific fracture energy. The primed quantities show the dynamic constitutive parameters.

The strain-rate sensitivity of fracture energy is applied through a dynamic magnification factor DMF_f, so that:

$$G'_f = DMF_f G_f \quad (7)$$

Failure criterion: The strength of concrete under multi-axial stresses is a function of the state of stress and cannot be predicted by limitation of simple tensile, compressive and shearing stresses independently of each other. In the elasticity based models, a suitable failure criterion is incorporated for a complete description of the ultimate strength surface. Criteria such as yielding, load carrying capacity and initiation of cracking have been used to define failure (Babu *et al*., 2005). Many failure criterions have been proposed for brittle material as well as concrete. Some of more familiar criterions are Mohr-Coulomb criteria, Drucker-Prager, Chen and Chen (1975), Ottosen (1977), Hsieh *et al*. (1982), Willam and Warnke (1974), Menetrey and William (1995), Sankarasubramanian and Rajasekaran (1996) and Fan and Wang (2002).

In the present study an advanced failure criterion is used for initiation and propagation of cracks in concrete structural components (Menetrey and William, 1995). In the general form this yield function can be expressed as follow:

$$f(\xi,\rho,\theta)=\left[\sqrt{\frac{3}{2}}\frac{\rho}{f_c'}\right]^2+m\left[\frac{\rho}{\sqrt{6}f_c'}r(\theta,e)+\frac{\xi}{\sqrt{3}f_c'}\right]-c=0 \quad (8)$$

where, ξ is hydrostatic stress invariant, ρ is deviatory stress invariant, θ is deviatory polar angle, r (θ, e) is an elliptic function, e describes the shape of the deviatory trace, m represents the frictional resistance of material, c is cohesion of material and f'_c is uni-axial compressive strength of concrete. The main parameters in the above equation are defined as follow:

$$\begin{aligned}
&\xi=\frac{I_1}{\sqrt{3}},\ I_1=\sigma_{ii}\\
&\rho=\sqrt{2J_2},\ J_2=\frac{1}{2}S_{ij}S_{ji}\\
&\theta=\frac{1}{3}\cos^{-1}\left(\frac{3\sqrt{3}}{2}\frac{J_3}{J_2^{3/2}}\right),\ J_3=\frac{1}{3}S_{ij}S_{jk}S_{ki}
\end{aligned} \quad (9)$$

where, I_1 is the first invariant of the Cauchy stress tensor; J_2 and J_3 are the second and third invariants of the deviatory part of the Cauchy stress tensor; σ_{ii} is principal stress; S_{ij}, S_{ji}, S_{jk} and S_{ki} are deviatory stresses. In addition, the elliptic function is in the form of Eq. 10, as following:

$$r(\theta,e)=\frac{4(1-e^2)\cos^2\theta+(2e-1)^2}{2(1-e^2)\cos\theta+(2e-1)\left[4(1-e^2)\cos^2\theta+5e^2-4e\right]^{1/2}} \quad (10)$$

FORMULATION OF FLUID-STRUCTURE-INTERACTION

The general coupled equation of motion for Fluid-structure-interaction (FSI) under dynamic loads is

discussed in this section. Considering the coupled dam-reservoir-foundation system, the governing equation in the reservoir medium is Helmholtz equation from the Euler's equation given as Ghaemian *et al.* (2003):

$$\nabla^2 p = \frac{1}{C^2}\frac{\partial^2 p}{\partial t^2} \quad (11)$$

where, p, C and t are the hydrodynamic pressure, pressure wave velocity in liquid and time, respectively. Boundary conditions required to apply on the reservoir medium to solve Eq. 11 are explained Hariri-Ardebili and Mirzabozorg (2010). The equations of the dam-foundation (as the structure) and the reservoir take the form:

$$\begin{bmatrix} [M] & 0 \\ \rho[Q]^T & [G] \end{bmatrix}\begin{Bmatrix} \ddot{U} \\ \ddot{P} \end{Bmatrix} + \begin{bmatrix} [C] & 0 \\ 0 & [C'] \end{bmatrix}\begin{Bmatrix} \dot{U} \\ \dot{P} \end{Bmatrix} + \begin{bmatrix} [K] & -[Q] \\ 0 & [K'] \end{bmatrix}\begin{Bmatrix} U \\ P \end{Bmatrix} = \begin{Bmatrix} \{f_1\} - [M]\{\ddot{U}_g\} \\ \{F\} - \rho[Q]^T\{\ddot{U}_g\} \end{Bmatrix} \quad (12)$$

where, [M], [C] and [K] are the mass, damping and stiffness matrices of the structure including the dam body and its foundation media and [G], [C'] and [K'] are matrices representing the mass, damping and stiffness equivalent matrices of the reservoir, respectively. The matrix [Q] is the coupling matrix; $\{f_1\}$ is the vector including both the body and the hydrostatic force; {P} and {U} are the vectors of hydrodynamic pressures and displacements, respectively and {Ug} is the ground acceleration vector.

FINITE ELEMENT MODELING AND CASE STUDIES

In order to investigate the ability of proposed method in static and dynamic analysis of concrete structural components two kinds of models were developed. The first one is a simple notched beam under three-point bending test and the second one is coupled prototype gravity dam-reservoir-foundation system under a combination of various load types. Figure 2 shows the model used for the three-point bending test. It's a square-section concrete beam with an initial notch depth of 51 mm in its center while the depth of the beam is 102 mm (Malvar and Warren, 1988). The material properties are as follow; E = 21.7 GPa, ν = 0.2, f'_t = 2.4 MPa, f'_c = 29.0 MPa and G_f = 35 N m^{-1}. Finite element model of half of concrete beam with fine mesh is also depicted in Fig. 2.

Figure 3 shows the finite element model and also dimension of prototype gravity dam-reservoir-foundation system. The model consists of solid elements for simulation of body and mass-less foundation and also fluid elements for modeling the reservoir. Boundary

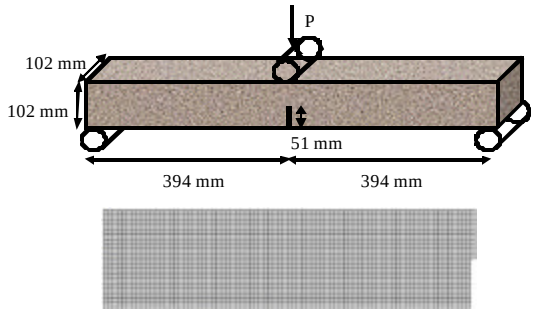

Fig. 2: Geometry and finite element model of single-edge-notched beam subjected to three point bending test

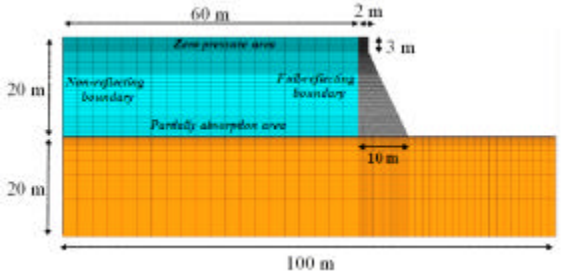

Fig. 3: Finite element model, dimensions and boundary conditions in coupled system

conditions are also depicted in this Fig. 3. Material properties of mass concrete in static and dynamic conditions are as follow; Modulus of elasticity is 40 and 46 GPa, Poisson's ratio is 0.2 and 0.14, density is 2640 kg m^{-3}, tensile strength is 2 MPa and dynamic tensile stress is 3 MPa. Modulus of elasticity in foundation area is 30 GPa and Poisson's ratio is 0.2. Sound velocity in water is assumed to be 1460 m sec^{-1}.

Three types of dynamic loads were used in present study, i.e., intensifying sinusoidal loading, increasing step loading and real earthquake ground motion. The two first load types were selected to investigation the pattern, route and the type of cracking of huge mass concrete specimen under dynamic loads including fluid-structure interaction. Acceleration time-histories of all three loads are depicted in Fig. 4a-c. Damping was assumed to be 10% of critical damping in all cases.

RESULTS AND DISCUSSION

Verification of proposed model: In Fig. 5, the load versus load-point deflection curves from the finite element model is compared with the experimental result of Malvar and Warren (1988). Two type of smeared crack were assumed

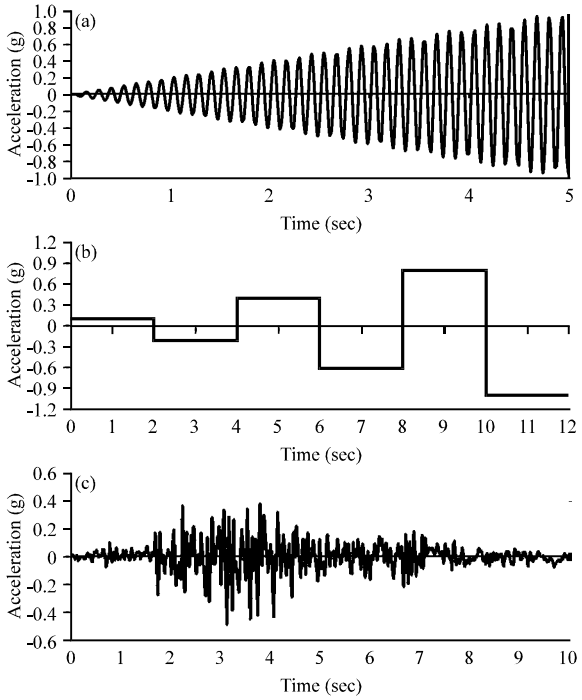

Fig. 4(a-c): Acceleration time-histories applied to the coupled system (a) Intensifying sinusoidal load, (b) Increasing step load and (c) Real earthquake ground motion

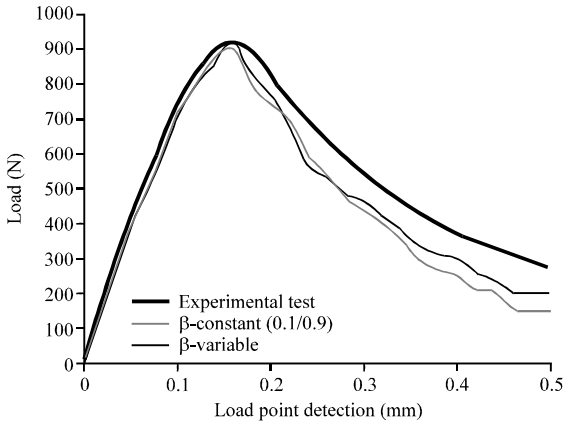

Fig. 5: Load versus load-point deflection compared with the experimental result for constant and variable shear transfer coefficients

for each beams, i.e., in the first approach shear transfer coefficient is assumed to have two constant parameters for open and closed cracks and in the second case variable shear transfer coefficient is take into account in smeared crack model. In the constant coefficient approach the pre-assumed values in open and cracked conditions

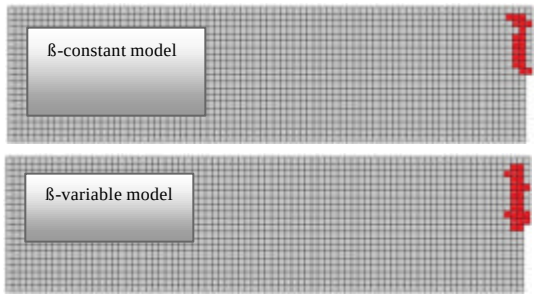

Fig. 6: Final crack profile in concrete beam under the concentrated load at the middle span

are 0.1 and 0.9, respectively. There is good agreement between predictions of the two approaches through all loading stages: elastic, hardening and softening. The numerical results also agree very well with the experimental result which demonstrates the soundness of the present algorithm. The final crack profiles of concrete beam are shown in Fig. 6. Although, the general pattern of crack profiles based on constant and variable shear transfer coefficients are close to each other, some differences can be shown in final crack profile. The crack is started from upper parts of the notch near the corner and extended almost linearly toward the upper edge of the beam.

Concrete dam model and FSI problem: In this section application of proposed smeared crack model is investigated for the problems consisting fluid-structure-interaction. For this purpose the introduced coupled system in previous section is selected as case study. The modeled concrete structure is assumed to be a prototype of a concrete gravity dam, its support assumed to be modeling of foundation rock and finally the fluid is considered as reservoir water.

So the dam-reservoir-foundation system is subjected to various types of loading as mentioned before. In each case the nonlinear responses of the system are compared with reference linear responses. Three nonlinear models are considered for each loading in which the first two ones use constant shear transfer coefficients for open and closed cracks and the third one uses proposed rotating smeared crack model with ability of updating shear transfer coefficient in each load step of dynamic analysis.

Intensifying sinusoidal loading: In this section the results of coupled system under an intensifying sinusoidal loading are investigated. The values of shear transfer coefficients for open and close cracks were assumed to be

0.1 and 0.9 in the first case and 0.3 and 0.7 in the second one. Figure 7 shows the time-history of crest displacement in stream direction for various linear and nonlinear models. As it is clear using nonlinear model based on smeared crack model lead to higher displacements than to linear one. Because of continuously intensifying nature of this loading the behavior of system gradually goes from linear elastic range to nonlinear phase and finally leads to global instability of the coupled system.

Based on this Fig. 7 up to time t = 1.36 sec all models show the same behavior which shows that models are in linear elastic range. After t = 1.36 sec the nonlinear behavior of models are begin in the form of concrete cracking. All three models have different behavior showing the importance of shear transfer coefficient in nonlinear analyses. The β-constant (0.1/0.9 values) model fails earliest at the time t = 4.14 sec showing that in the current model, assuming value near unit for shear transfer coefficient in closed cracks condition and value near zero in open cracks condition can lead to unrealistic results. The β-constant (0.3/0.7 values) model is the second one which fails under the same loading at time t = 4.28 sec. Although this models endure more than previous one under intensifying loading, it has limitations for fully capture the nonlinear behavior of concrete under dynamic loading. The third model in which β varies based on the proposed model, experiences some large deformations up to 28 mm in first 5 sec of dynamic load. However, there is no global instability in this case.

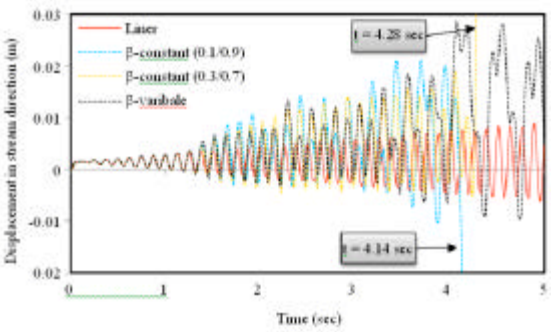

Fig. 7: Crest displacement under intensifying sinusoidal dynamic load for linear and nonlinear models

Figure 8a-d represent the non-concurrent envelope of the first principal stress within the dam body. As it is shown, considering that there is no limitation in linear model its stresses are increased to 12.7 MPa which is mainly concentrated near the toe and heel of base. Using nonlinear models concentrate the area with high tensile stress in dam-foundation interface and also some areas around the neck. Consequently theses areas have great capability for cracking. The similarity of β-variable model to β-constant (0.1/0.9 values) is more than β-constant (0.3/0.7 values). Figure 9a-c show the propagation of crack profile by increasing the intensity of loading for nonlinear

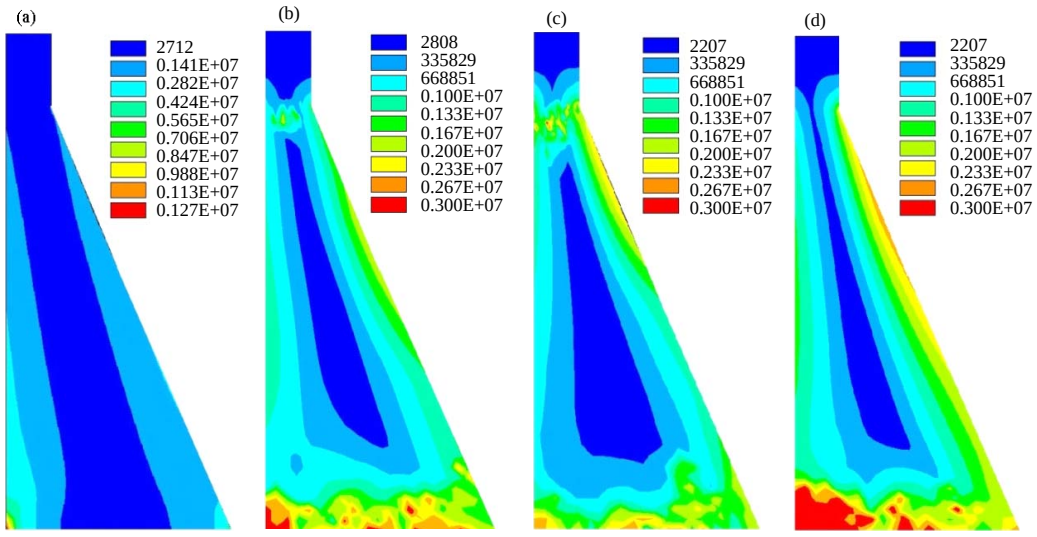

Fig. 8(a-d): Non-concurrent envelope of first principal stresses in dam body (a) Linear model, (b) β-variable model, (c) β-constant-(0.1/0.9) and (d) β-constant-(0.3/0.7)

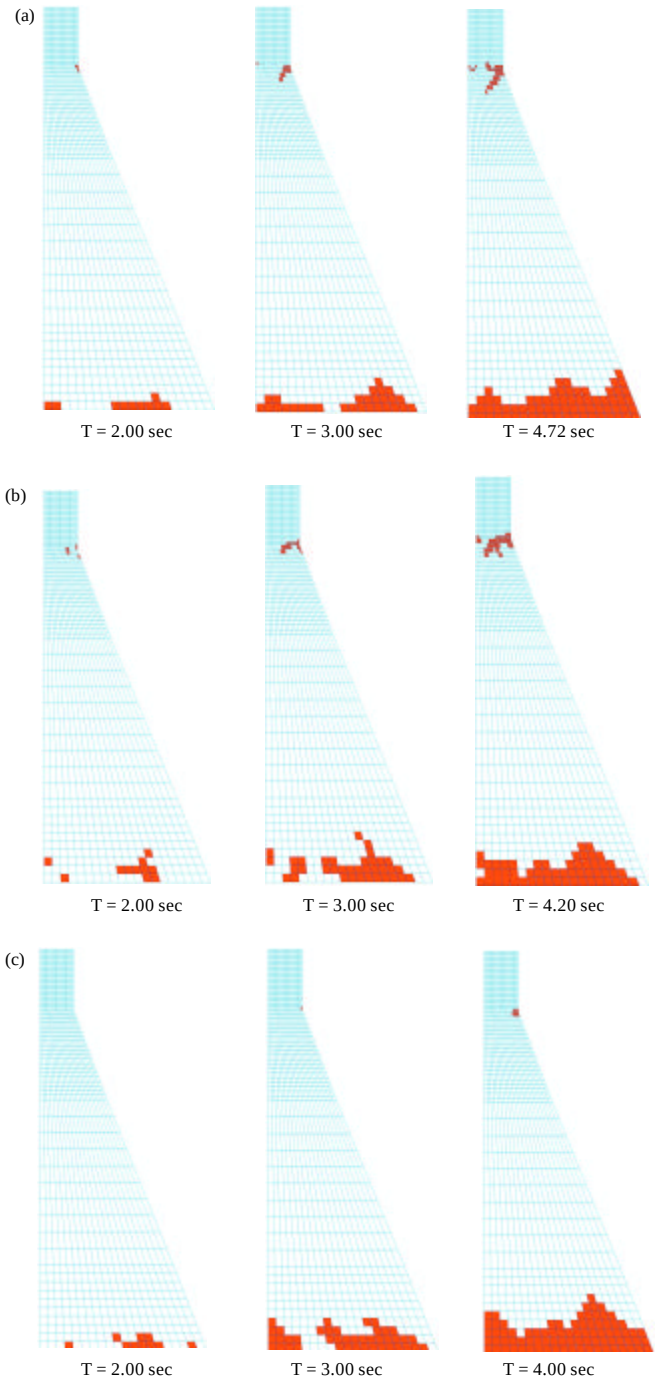

Fig. 9(a-c): Crack propagation in dam body and final crack profile in failure time (a) β-variable model, (b) β-constant-(0.1/0.9) and (c) β-constant-(0.3/0.7)

models. Also the final crack profiles are shown in this figure. As can be seen at t = 2.00 sec almost all models have close crack profiles and at t = 3.00 sec β-variable and β-constant (0.1/0.9 values) models have considerable

cracked element in neck area. For the final crack profiles all models show complete cracking in base of the dam and in neck area.

Increasing step loading: This sub-section is provides the responses of dam-reservoir-foundation system under increasing step-type loading. This load type is similar to previous one by this way that both is increasing and is different from that one considering that it applies acceleration to system which is not damps rapidly. Figure 10 shows time-history of crest displacement in stream direction for linear and nonlinear models. As can be seen using linear model generate uniform displacement curve similar to input acceleration while the damping of acceleration in the system is clearly recognizable. Based on these results the coupled system damps the input acceleration in time interval about 0.33 sec. Comparing the nonlinear models shows that β-variable model fails at t = 6.14 sec while using β-constant-(0.1/0.9) leads to failure of the system at t = 8.08 sec, respectively. In addition based on β-constant-(0.1/0.9) model, the damping of input acceleration in nonlinear phase is done very slowly.

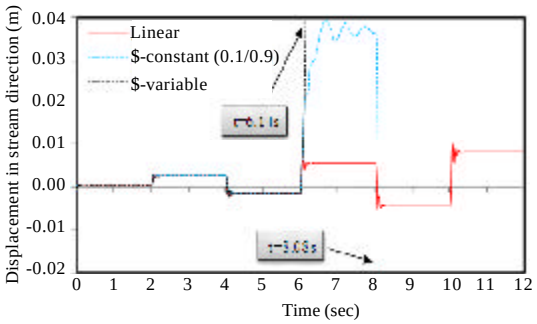

Fig. 10: Crest displacement under increasing step-type dynamic load for linear and nonlinear models

Figure 11a-c represent the non-concurrent envelope of first principal stress within the dam body under spet-type loading. As it is shown considering that there is no limitation in linear model its stresses are increased to 11.92 MPa which is mainly concentrated near the toe and heel of base and also in middle parts of upstream face. The stress envelopes of variable and constant shear transfer coefficients are very close to each other, while β-constant-(0.1/0.9) model generates more high stress areas in base of dam. Figure 12a and b show the propagation of crack profile at different times for nonlinear models. As can be seen the final crack profile for the β-variable model at time 8.94 sec and β-constant (0.1/0.9 values) model at t = 8.54 sec are almost the same. In addition for the lower times β-constant model generates more damage in base of dam. There is no crack in neck area under this type of loading.

Real ground motion loading: Figure 13 shows time-history of crest displacement for linear and nonlinear models using real ground motion. As can be seen because moderate intensity of selected ground motion none of

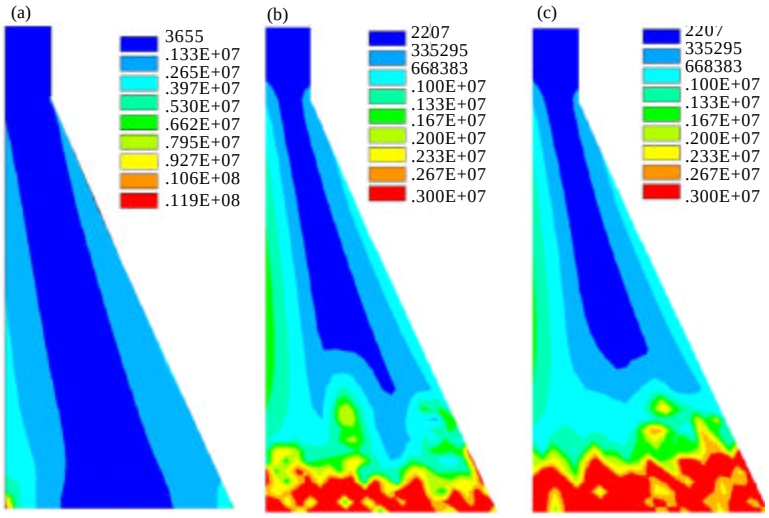

Fig. 11(a-c): Non-concurrent envelope of first principal stresses in dam body (a) Linear model; (b) β-variable model and (c) β-constant-(0.1/0.9)

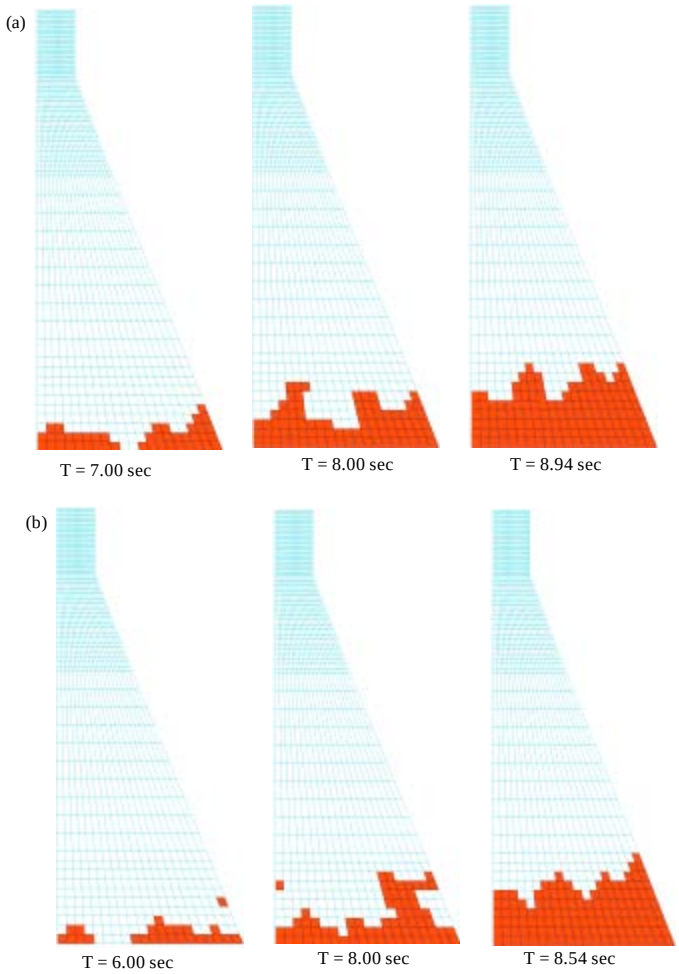

Fig. 12(a-b): Crack propagation in dam body and final crack profile in failure time (a) variable model and (b) constant-(0.1/0.9)

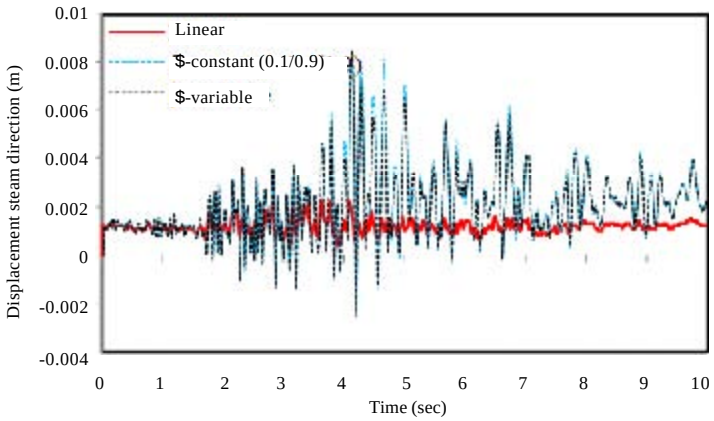

Fig. 13: Crest displacement under real ground motion for linear and nonlinear models

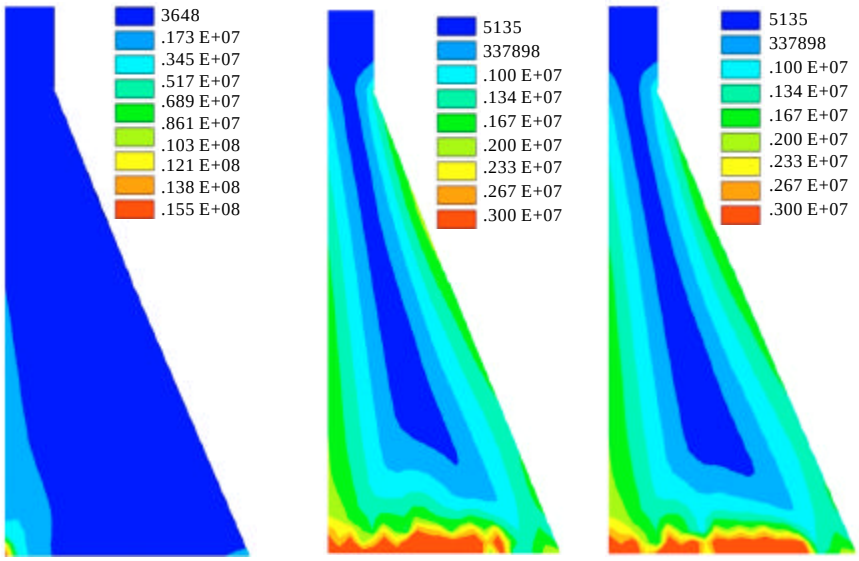

Fig. 14(a-c): Non-concurrent envelope of first principal stresses in dam body (a) Linear model, (b) β-variable model and (c) β-constant-(0.1/0.9)

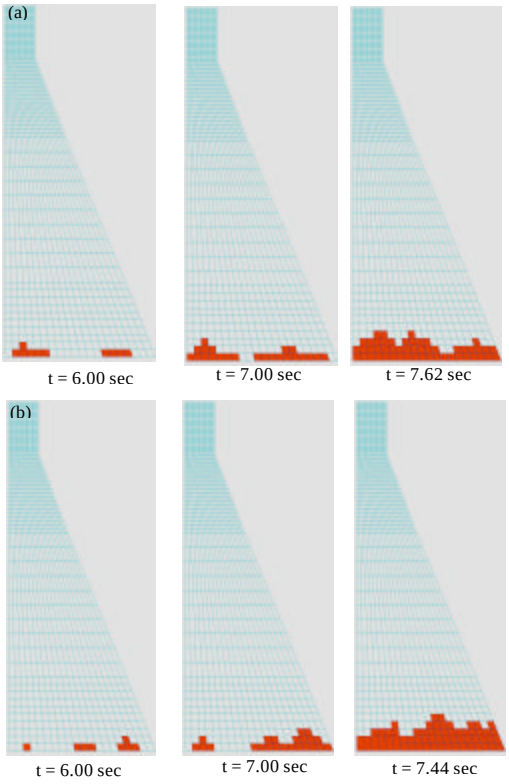

Fig. 15(a-b): Crack propagation in dam body and final crack profile in failure time (a) β-variable model and (b) β-constant-(0.1/0.9)

nonlinear-based models were failed. Although, both nonlinear models generate larger values for displacement that to linear model, using β-constant-(0.1/0.9) model leads to some larger displacement that to β-variable model and two models have great consistency with each other.

Figure 14a-c represent the non-concurrent envelope of first principal stress within the dam body under real ground motion. Linear model experiences up to 15.53 MPa tensile stress in toe of dam. The general templates of two nonlinear models are very close each other and overstressed area is concentrated in base of dam at vicinity of foundation. Figure 15a and b shows the propagation of crack profile for nonlinear models under real ground motion. In spite of the previous load types, there is no continuously increasing loading in this example. Like the Fig. 13 and 14, there is great similarity between crack profiles not only for the final profiles but also the propagation of crack based on two approaches have almost same trend.

CONCLUSION

In the present study a co-axial rotating smeared crack model was introduced for nonlinear behavior of mass concrete in 3D space. The advantages of proposed model are; using variable shear transfer coefficient which is updated in each load step; utilizing an advanced failure criterion for concrete in 3D space and ability of this method in simulation of cracking process in concrete with

high accuracy. The proposed model was verified using the three-point bending test of concrete beam. Results show very good consistency between numerical analysis and experimental test. On the other hand, finite element model of prototype gravity dam-reservoir-foundation system was provided in order to investigation the nonlinear dynamic behavior of large concrete specimens considering fluid-structure-interaction. Three types of dynamic loading were selected for this purpose; i.e., two increasing loads and one real ground motion record. The results were compared for constant and proposed variable shear transfer coefficients. It was found that generally shear transfer coefficient affects the results of dynamic analysis of concrete structures meaningfully. In high intensity levels of dynamic load, constant shear transfer coefficient leads to early failure of structure than to variable coefficient model. Also both final crack profile and the propagation of cracks within concrete specimens are highly affected by shear transfer coefficient. Finally it was concluded that the proposed model can be used for static and dynamic crack analysis of concrete structural components considering the effects of fluid-structure-interaction and hydrodynamic pressure on specimen.

REFERENCES

Ahmadi, M.T. and S. Razavi, 1992. A three dimensional joint opening analysis of an arch dam. Comput. Struct., 44: 187-192.

Ahmadi, M.T., M. Izadinia and H. Bachmann, 2001. A discrete crack joint model for nonlinear dynamic analysis of concrete arch dam. Comput. Struct., 79: 403-420.

Ardakanian, R., M. Ghaemian and H. Mirzabozorg, 2006. Nonlinear behavior of mass concrete in 3-D problems using damage mechanics approach. Eur. Earthquake Eng., 2: 65-89.

Babu, R.R., G.S. Benipal and A.K. Singh, 2005. Constitutive modeling of concrete: An overview. Asian J. Civil Eng. Build. Hous., 6: 211-246.

Chen, A.C.T. and W.F. Chen, 1975. Constitutive relations for concrete. J. Eng. Mech. Div., 101: 465-481.

Cicekli, U., G.Z. Voyiadjis and R.K. Abu Al-Rub, 2007. A plasticity and anisotropic damage model for plain concrete. Int. J. Plast., 23: 1874-1900.

Contrafatto, L. and M. Cuomo, 2006. A framework of elastic-plastic damaging model for concrete under multiaxial stress states. Int. J. Plast., 22: 2272-2300.

Du, X. and J. Tu, 2007. Nonlinear seismic response analysis of arch dam-foundation systems-part II opening and closing contact joints. Bull. Earthquake Eng., 5: 121-133.

Fan, S.C. and F. Wang, 2002. A new strength criterion for concrete. Struct. J., 99: 317-326.

Ghaemian, M., A.R. Khaloo and H. Mirzabozorg, 2003. Staggered solution scheme for three-dimensional analysis of dam-reservoir interaction. Dam Eng. J., 14: 1-33.

Grassl, P. and M. Jirasek, 2006. Damage-plastic model for concrete failure. Int. J. Solids Struct., 43: 7166-7196.

Hariri-Ardebili, M.A. and H. Mirzabozorg, 2010. Numerical Simulation of Reservoir Fluctuation Effects on Nonlinear Dynamic Response of Concrete Arch Dams, Advance Fluid Mechanics VIII (AFM). WIT Press, Algarve, Portugal, pp: 427-438.

He, W., Y.F. Wu, K.M. Liewand and Z. Wu, 2006. A 2D total strain based constitutive model for predicting the behaviors of concrete structures. Int. J. Eng. Sci., 44: 1280-1303.

Hohberg, J.M., 1990. A note on spurious oscillations in FEM joint elements. Earthquake Eng. Struct. Dyn., 19: 773-779.

Hsieh, S.S., E.C. Ting and W.F. Chen, 1982. A plastic-fracture model for concrete. Int. J. Solids Struct., 18: 181-197.

Khan, A.R., A.H. Al-Gadhib and M.H. Baluch, 2007. Elasto-damage model for high strength concrete subjected to multiaxial loading. Int. J. Damage Mech., 16: 361-398.

Labadi, Y. and N.E. Hannachi, 2005. Numerical simulation of brittle damage in concrete specimens. Strength Mater., 37: 268-281.

Lotfi, V. and R. Espandar, 2004. Seismic analysis of concrete arch dams by combined discrete crack and non-orthogonal smeared crack technique. Eng. Structures, 26: 27-37.

Malvar, L.J. and G.E. Warren, 1988. Fracture energy for three-point-bend tests on single-edge-notched beams. Exp. Mech., 28: 266-272.

Malvar, L.J. and M.E. Fourney, 1990. A three dimensional application of the smeared crack approach. Eng. Fract. Mech., 35: 251-260.

Menetrey, P. and K.J. William, 1995. Triaxial failure criterion for concrete and its generalization. ACI Struct. J., 92: 311-318.

Mirzabozorg, H. and M. Ghaemian, 2005. Nonlinear behavior of mass concrete in three-dimensional problems using smeared crack approach. Earthquake Eng. Struct. Dyn., 34: 247-269.

Mirzabozorg, H., A.R. Khaloo, M. Ghaemian and B. Jalalzadeh, 2007. Non-uniform cracking in smeared crack approach for seismic analysis of concrete dams in 3D space. Int. J. Earthquake Eng. Seism., 2: 48-57.

Mirzabozorg, H., M. Ghaemian and M.R. Kianoush, 2004. Damage mechanics approach in seismic analysis of concrete gravity dams including dam-reservoir interaction. Eur. Earthquake Eng., 18: 17-24.

Mirzabozorg, H., M.R. Kianoush and M. Varmazyari, 2010. Nonlinear behavior of concrete gravity dams and effect of input spatially variation. Struct. Eng. Mech., 35: 365-379.

Mosler, J. and G. Meschke, 2004. Embedded crack vs. smeared crack models: A comparison of elementwise discontinuous crack path approaches with emphasis on mesh bias. Comput. Methods Applied Mech. Eng., 193: 3351-3375.

Ottosen, N.S., 1977. A failure criterion for concrete. J. Eng. Mech. Div., 103: 527-535.

Phama, H.B., R. Al-Mahaidia and V. Saouma, 2006. Modelling of CFRP-concrete bond using smeared and discrete cracks. Compos. Struct., 75: 145-150.

Sankarasubramanian, G. and S. Rajasekaran, 1996. Constitutive modeling of concrete using a new failure criterion. Comput. Struct., 58: 1003-1014.

Sumarac, D., M. Sekulovic and D. Krajcinovic, 2003. Fracture of reinforced concrete beams subjected to three point bending. Int. J. Damage Mech., 12: 31-44.

Weihe, S., B. Kroplin and R. de Borst, 1998. Classification of smeared crack models based on material and structural properties. Int. J. Solids Struct., 35: 1289-1308.

Willam, K.J. and E.P. Warnke, 1974. Constitutive Model for Triaxial Behavior of Concrete. International Association for Bridges and Structure Engineering, Italy.

Yu, R.C., G. Ruiz and E.W.V. Chaves, 2008. A comparative study between discrete and continuum models to simulate concrete fracture. Eng. Fracture Mech., 75: 117-127.